Polymer 51 (2010) 53–61

Contents lists available at ScienceDirect

Polymer

journal homepage: www.elsevier.com/locate/polymer

Ring-opening metathesis polymerization (ROMP) of norbornenyl-functionalized fatty alcohols

Ying Xia, Yongshang Lu, Richard C. Larock*

Department of Chemistry, Iowa State University, Ames, IA 50011, United States

ARTICLE INFO

Article history:
Received 10 September 2009
Received in revised form
5 November 2009
Accepted 7 November 2009
Available online 15 November 2009

Keywords:
ROMP
Thermoset
Biorenewable

ABSTRACT

Novel biorenewable-based thermosets have been successfully synthesized by the ring-opening metathesis polymerization (ROMP) of norbornenyl-functionalized fatty alcohols derived from soybean oil (NMSA), Dilulin (NMDA), ML189 (NMMA) and castor oil (NMCA). The effects of the monomer structure on the polymerization process, and the thermal and mechanical properties of the resulting thermosets have been extensively investigated. The number of ROMP-reactive rings appended to the fatty acid chain and the viscosity play an important role in controlling the initiation and propagation processes of the polymerization and the final properties of the thermosets obtained. The thermosets have been characterized by Soxhlet extraction, DMA, TGA, and tensile tests. It has been found that polyNMDA and polyNMMA have best thermo-mechanical properties. Compared with polyNMSA, the polyNMDA and polyNMMA thermosets exhibit lower soluble fractions, and higher thermal stabilities and mechanical properties, because of more effective crosslinking; whereas, polyNMCA exhibits a higher soluble fraction, and lower thermal stability, resulting from incomplete polymerization of the more viscous NMCA monomer.

Published by Elsevier Ltd.

1. Introduction

Bio-based materials have attracted much attention because of their sustainability and environmental concerns [1]. Recently, renewable materials synthesized from plant products have shown great promise as a replacement for petroleum-based materials [2]. Thermosetting resins [3], biodegradable polymers [4], biocomposites [5] and polyurethane dispersions [6,7] from acylated epoxidized soybean oil, soy protein and vegetable oil-based polyols have been successfully synthesized by free radical, ring-opening and addition polymerizations. In our previous work, we have taken advantage of the carbon-carbon double bonds in soybean [8], linseed [9], tung [10], corn [11] and fish [12] oils to develop a variety of new polymeric materials by cationic or thermal copolymerization of these natural oils with styrene (ST) and divinylbenzene (DVB). The resulting thermosetting polymers can be varied from elastomers to tough and rigid plastics by simply changing the stoichiometry, and the nature of the oil and alkene comonomers. These new polymers exhibit thermophysical and mechanical properties that are comparable to those of commercially available elastomers and conventional plastics and may serve as replacements for petroleum-based polymers in many applications.

Olefin metathesis has also been employed in the synthesis of vegetable oil-based polymers, primarily through acyclic diene (triene) metathesis polymerization (ADMET/ATMET) [13,14] and ring-opening metathesis polymerization (ROMP) [15,16]. Recently, Meier et al. investigated the ADMET and ATMET bulk polymerizations of vegetable oil-based undecyl undecenoate and glyceryl triundec-10-enoate, respectively, using Grubbs' and Hoveyda–Grubbs' ruthenium catalysts, leading to high-molecular-weight triblock and branched polyesters [13,14]. Moreover, the molecular weight of the resulting polyesters can be controlled by adjusting the ratio of the monomer and the chain stopper in a one-step, one-pot procedure.

In our previous work, we reported the synthesis of vegetable oil-based polymers by ROMP, which is a powerful tool to convert cyclic olefins to various polymeric materials (see Scheme 1 for an example) [17]. In our work, two kinds of vegetable oil-based ROMP thermosetting polymers have been obtained successfully

* Corresponding author. Tel.: +1 5152944660; fax: +1 5152940105.
E-mail address: larock@iastate.edu (R.C. Larock).

0032-3861/$ – see front matter Published by Elsevier Ltd.
doi:10.1016/j.polymer.2009.11.011

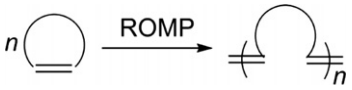

Scheme 1. A general example of ROMP.

by the copolymerization of Dilulin, a commercially available norbornene-modified linseed oil [18], with dicyclopentadiene (DCPD) [15] and a norbornene-functionalized castor oil (BCO) with cyclooctene [16] using Grubbs 2nd generation catalyst. Their good thermal and mechanical properties indicate great promise for these environmentally-friendly, vegetable oil-based materials as a new class of plastics. However, phase separations were observed in both the Dilulin/DCPD and BCO/cyclooctene thermosets, because of the large difference in reactivity between the vegetable oil-based monomers and the petroleum-based comonomers. The relatively low reactivity of the vegetable oil-based monomers can be attributed to their high viscosity and the free fatty acid chains, which may hinder coordination between the catalyst and the norbornene moiety present in the Dilulin and BCO. Similar results have also been observed in the vegetable oil-based thermosets from Dilulin and norbornene-based cross-linkers [19].

To address the phase separation, which occurred in the vegetable oil-based ROMP systems, while maintaining the good thermophysical and mechanical properties of the resulting polymers, in this work, four novel norbornenyl-functionalized fatty alcohols with different side chain structures have been successfully synthesized from soybean oil, Dilulin, ML189 and castor oil by first reducing the vegetable oil triglycerides to fatty alcohols, which were then reacted with 5-norbornene-2,3-dicarboxylate anhydride (see Scheme 2 for an example). These norbornenyl-functionalized biorenewable monomers can easily undergo ring-opening metathesis homopolymerization under Grubbs 2nd generation catalyst, leading to vegetable oil-based thermosets with good thermophysical and mechanical properties with no apparent phase separation.

2. Experimental section

2.1. Materials

Soybean oil was purchased at the local supermarket. Dilulin was supplied by Cargill (Chicago, IL). ML189 was obtained from Northern Sun, a division of Archer Daniels Midland (ADM) Company (Red Wing, MN). Castor oil, 5-norbornene-2,3-dicarboxylate anhydride (endo) and the 2nd generation Grubbs catalyst were purchased from Sigma-Aldrich (Milwaukee, WI). Lithium aluminum hydride (LAH) was purchased from Acros (Geel, Belgium). Benzene, ethyl acetate, methylene chloride and hydrochloric acid were obtained from Fisher (Fair Lawn, NJ). Tetrahydrofuran (THF) was distilled over sodium/benzophenone under N_2. Unless otherwise stated, all reagents were used as received without further purification.

2.2. Synthesis of norbornenyl-functionalized fatty alcohols

The synthesis of the norbornenyl-modified soybean alcohol (NMSA) is shown in Scheme 2. LAH (15.7 g, 0.41 mol) was dissolved in 100 mL of THF and stirred in a 500 mL two-neck round bottom flask. Soybean oil (120 g, 0.14 mol) was dissolved in THF (150 mL) and then added dropwise to the LAH solution. The reaction was carried out at 0 °C overnight. The reaction mixture was poured into ice water, followed by the addition of 1 M HCl, until the solution was clear. Then, 300 mL of ethyl acetate was added, resulting in two layers. The organic layer was washed with water to remove the glycerol, and then dried over $MgSO_4$ and filtered. Finally, the clear soybean alcohol was obtained after removal of the organic solvent under vacuum.

The soybean alcohol (50 g, 0.19 mol) was added to a 250 mL round bottom flask, and then 34.2 g (0.21 mol) of 5-norbornene-2,3-dicarboxylate anhydride (endo) was added, followed by 21.04 g (0.21 mol) of triethylamine. The mixture was stirred at 65 °C for 24 h and then diluted by the addition of 100 mL of ethyl acetate. The mixture was poured into a 1M aqueous HCl (400 mL) solution and stirred overnight to convert excess 5-norbornene-2,3-dicarboxylate anhydride to water soluble 5-norbornene-2,3-dicarboxylic acid.

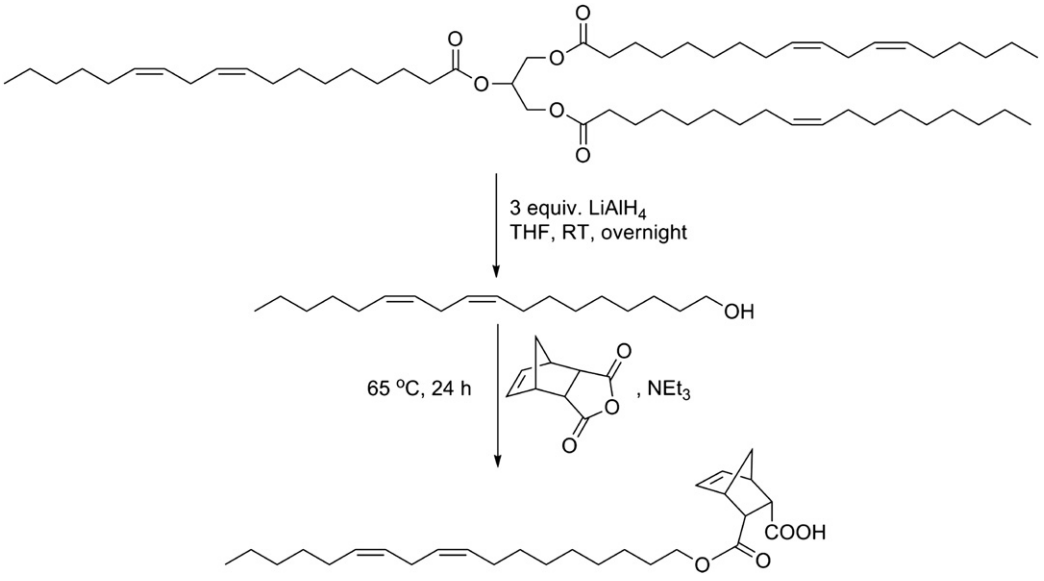

Scheme 2. Synthesis of norbornenyl-modified soybean alcohol (NMSA).

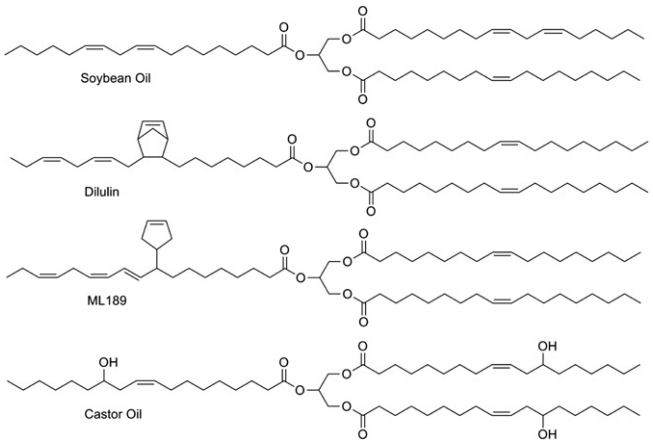

Scheme 3. Representative chemical structures of soybean oil, Dilulin, ML189 and castor oil.

Then the mixture was extracted by ethyl acetate, washed by 1 M HCl and brine, and dried over $MgSO_4$. After evaporating the solvent under vacuum, a near quantitative yield of endo-norbornenyl-modified soybean alcohol (NMSA) was obtained (see later for peak assignments and integration in ^{1}H NMR).

The other vegetable oil-based monomers, norbornenyl-modified Dilulin alcohol (NMDA), norbornenyl-modified ML189 alcohol (NMMA) and norbornenyl-modified castor oil (NMCA) were synthesized and purified using the same method as that mentioned above.

2.3. Freeze-drying of the Grubbs catalyst

To improve the solubility of the Grubbs catalyst in the monomers, freeze-drying of the catalyst was carried out according to a literature procedure [20]. The 2nd generation Grubbs catalyst (250 mg) was dissolved in 5 mL of benzene and the solution was frozen in a liquid nitrogen bath. The frozen sample was then placed in a vacuum oven at room temperature for 5 h to sublime the benzene. This process provided catalyst with larger surface areas.

2.4. Polymerization

Ten grams of monomer was weighed into a PTFE-coated 20 mL vial. Freeze-dried Grubbs 2nd generation catalyst (50 mg, 0.5 wt%) was mixed with the monomer using a spatula until all of the catalyst was dissolved and a homogeneous solution was obtained. The mixture was heated at 65 °C for 1 h and 150 °C for 3 h. The resulting thermosets were slightly transparent and retain the oil's original color.

2.5. Soxhlet extractions

A 2–3 g sample of the bulk polymer was extracted with 100 mL of refluxing methylene chloride for 24 h using a Soxhlet extractor. Following extraction, the resulting solution was concentrated under reduced pressure and dried in a vacuum oven at 60 °C overnight.

2.6. Characterization

^{1}H NMR spectroscopic analysis of the monomers and the soluble substances extracted from the thermosets by methylene chloride were recorded in $CDCl_3$ using a Varian spectrometer (Palo Alto, CA) at 300 MHz.

The viscosities of the monomers were measured with a cone (1°, 40 mm diameter) and detachable sample plate on an AR2000ex (TA Instruments, New Castle, DE) at 25 °C, while the shear rate was increased from 0 to 500 s^{-1}. The gelation time was also determined on the AR2000ex by applying an oscillating strain to the sample and measuring the response stress. All experiments were performed at 65 °C, using stress control mode at 1 Hz, with 25 mm diameter disposable parallel plates and a 0.5 mm gap.

Differential scanning calorimetry (DSC) cure analyses of the monomers were recorded on a TA Instruments Q20. Monomers were mixed with the Grubbs 2nd generation catalyst, and then the mixtures were transferred to an aluminum DSC pan and loaded into the DSC chamber immediately. The samples were scanned from −50 °C to 240 °C at a heating rate of 10 °C/min.

The dynamic mechanical analyses (DMA) was recorded on a TA Instruments Q800 dynamic mechanical analyzer using a three-point bending mode at 1 Hz. Rectangular samples 1.5 mm thick and

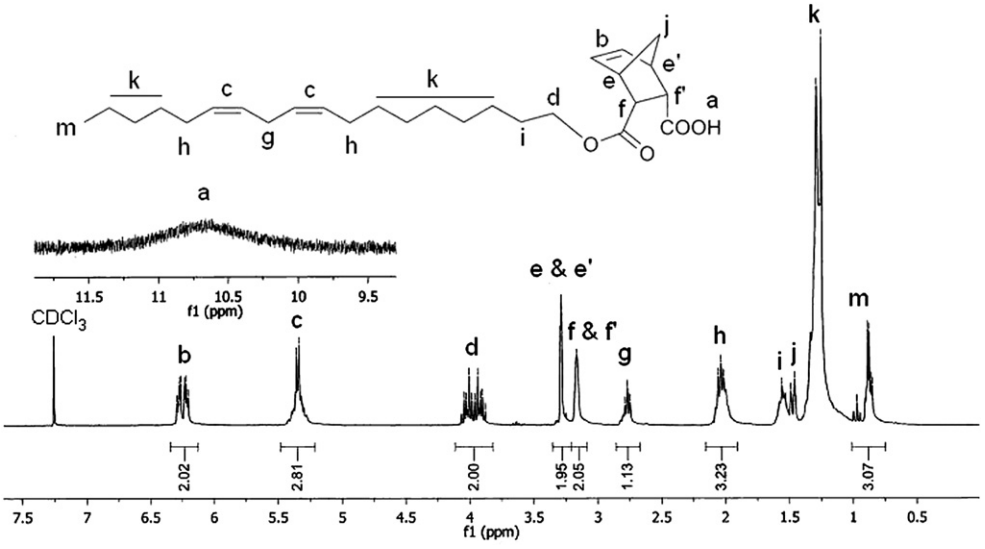

Fig. 1. ^{1}H NMR spectra of NMSA.

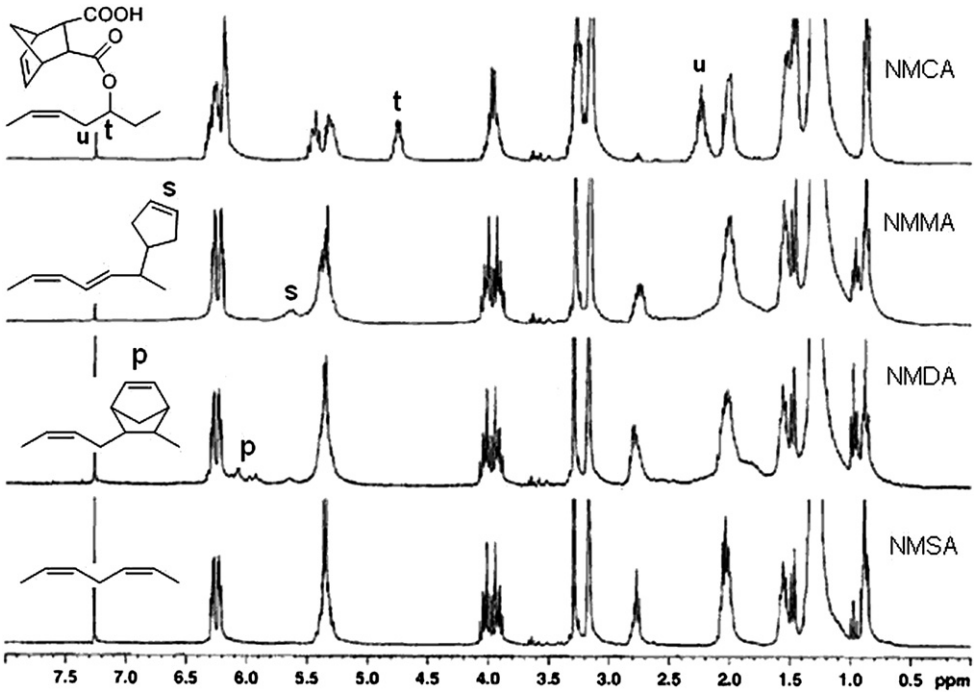

Fig. 2. ^{1}H NMR spectra of NMSA, NMDA, NMMA and NMCA.

10 mm wide were used for the analysis. Samples were cooled and held isothermally for 3 min at −80 °C before the temperature was increased at 3 °C/min to 200 °C.

Thermogravimetric analysis (TGA) of the specimens was carried out on a TA Instruments (New Castle, DE) Q50. Samples were scanned from 50 °C to 650 °C in air with a heating rate of 20 °C/min.

The mechanical properties of the thermosets were determined using an Instron universal testing machine (model 4502) with a crosshead speed of 50 mm/min. Rectangle specimens of $70 \times 10 \times 3$ mm^3 (length × width × thickness) were used. An average value of five replicates of each sample was taken. The toughness of the polymer, which is the fracture energy per unit volume of the sample, was obtained from the area under the corresponding tensile stress-strain curves.

3. Results and discussion

3.1. Monomer characterization

Structures representative of the commercially available vegetable oils employed in this study are shown in Scheme 3. Soybean oil is a triglyceride structure consisting of mainly unsaturated oleic, linoleic and linolenic fatty acids [21]. Dilulin and ML189 are linseed oil-based commercial industrial oils with complex components,

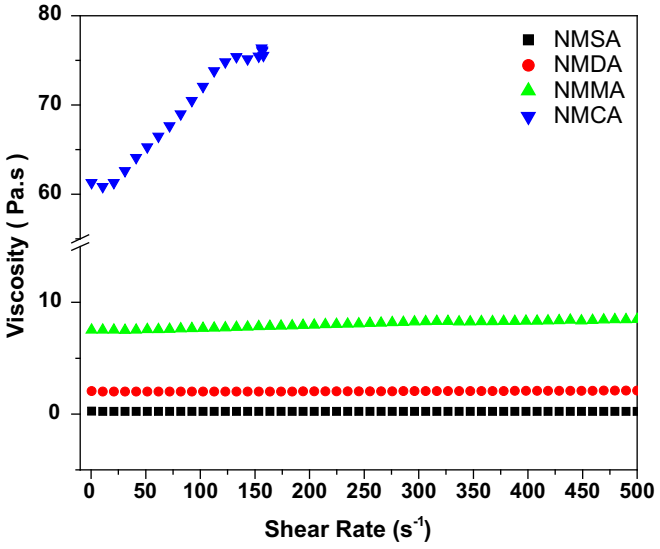

Fig. 3. Viscosities of the monomers.

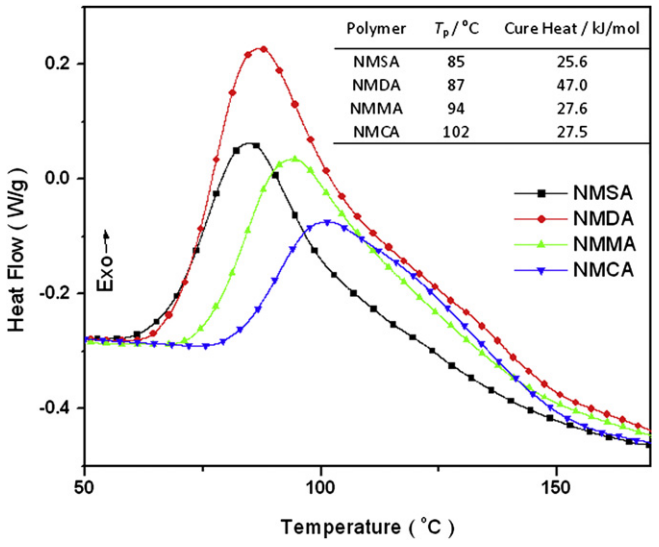

Fig. 4. Curing kinetic curves for the monomers.

which have been characterized before [22]. Dilulin with approximately one norbornene ring per triglyceride is prepared by the Diels–Alder reaction between linseed oil and cyclopentadiene under high temperature and pressure [18], while ML189 is also a dicyclopentadiene-modified linseed oil [23], which appears to contain approximately one cyclopentene ring per triglyceride. The ROMP of Dilulin or ML189 results in soft, but weak, polymers, which indicates that the rings appended onto the fatty acid chains can be ring-opened to form polymers. Castor oil, consisting of approximately ninety percent ricinoleic acid, has about 2.7 hydroxyl groups per triglyceride [16]. The variety of fatty acid chains present in these oils makes it possible to vary the nature of the monomer and examine the properties of the resulting thermosets.

Fig. 1 shows the detailed ^{1}H NMR spectra of NMSA with integrations. The signals at 6.1–6.4 ppm (b) correspond to the norbornene protons, and the vinylic hydrogens of the fatty acid chains (c) are typically found at 5.2–5.5 ppm. The peaks centered at about 4.0 ppm (d) are attributed to the methylene protons close to the ester group of the monomer. Fig. 2 illustrates the ^{1}H NMR spectra for the four monomers and the new peaks not present in NMSA are assigned. Compared to NMSA, peaks at 5.9–6.1 (p) and 5.6 ppm (s) are observed in NMDA and NMMA, which are attributed to the norbornene and cyclopentene rings attached to the fatty acid chains in NMDA and NMMA, respectively. For the monomer NMCA, the tertiary hydrogen on the fatty acid chain is observed around 4.8 ppm (t) and a new methylene peak is seen at 2.2 ppm (u). These norbornenyl-modified fatty alcohols are suitable for ring-opening metathesis polymerization, due to the strained norbornene ring present in the monomer. For NMDA and NMMA, approximately one third of the fatty acid side chains are appended with a norbornene ring or a cyclopentene ring (calculated from the integration of the ^{1}H NMR spectra), which leads to crosslinking in the resulting thermosets. Compared with the other three monomers, 90% of NMCA has two norbornene rings, which should result in an even higher crosslink density.

3.2. ROMP of the monomers

In the ROMP initiation process using the 2nd generation Grubbs catalyst, the phosphine ligand first dissociates, then the olefin in the monomer coordinates to the reactive ruthenium center to initiate the polymerization process [24]. However, if the bulk monomer is too viscous, it may be more difficult to coordinate with the metal center, resulting in a slow initiation process and propagation of the polymerization [16]. Fig. 3 illustrates the viscosities of the four monomers. NMCA has a much higher viscosity than the other three monomers due to the stronger hydrogen bonding through the extra carboxylic acid groups. The relatively high viscosity of NMCA presumably prevents the movement of the monomer and this affects the initiation process and propagation of the polymerization process. Similar results have been reported previously [16].

Fig. 4 illustrates the peak temperatures (T_p) and cure heat for the curing kinetic curves of all four monomers. The T_ps increase as the viscosities of the monomers increase, which is in good agreement with the fact that the olefin in the monomer can coordinate to the ruthenium center more easily and thus initiate polymerization with the less viscous monomers. The exothermic peaks are due to the heat release from the strained rings present in the monomer and the cure heat was calculated based on the data obtained from DSC and molecular weight of the monomer. NMDA exhibits the largest cure heat of 47.0 kJ/mol which results from the additional norbornene ring in the monomer. However, NMMA containing an extra cyclopentene ring shows only a slightly higher cure heat than

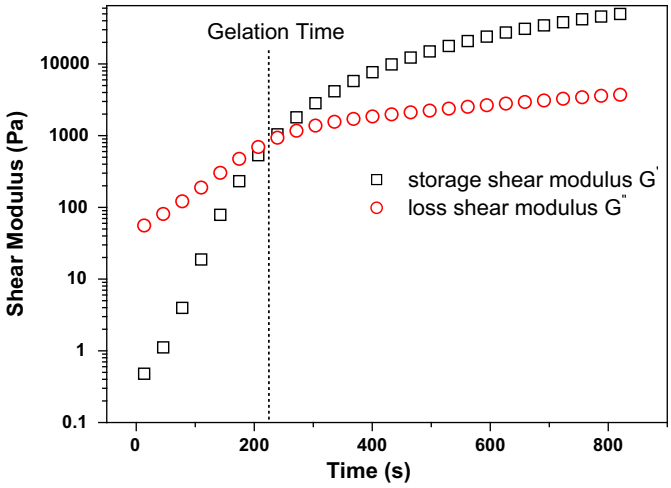

Fig. 5. Evolution of shear moduli during the reaction of the monomer/catalyst blend. Shown here is the NMDA/catalyst mixture curing at 65 °C.

NMSA. This can be explained by the fact that the cyclopentene rings present in the side chains of NMMA are less strained than the norbornene rings present in the side chains of NMDA. In addition, NMCA with nearly two norbornene rings exhibited lowest cure heat, probably due to incomplete polymerization of the NMCA monomers within the DSC scan time. More specifically, NMCA monomers having a much higher viscosity were constrained by strong hydrogen bonding between monomers, which significantly restricts the mobility of the monomer.

The gelation time for the four monomers was determined rheologically using a reported procedure [25]. Generally, the viscosity of the system increases dramatically when gelation occurs. A parallel plate oscillatory rheometer was used to measure the time dependence of the storage shear modulus, G', and the loss shear modulus, G'', for the monomer/catalyst mixture. As shown in Fig. 5, both G' and G'' increase gradually with time, the build-up rate of G' was much higher than that of G'' due to the formation of elastic polymers from chemical crosslinking. The differential in rates leads to a crossover of G' and G'', which is defined as the gel time, indicating the transition of the system from liquid phase dominated to a solid phase dominated viscoelastic behavior, also suggesting three-dimensional (3-D) network formation [26]. Table 1 summarizes the gelation time of the monomer/catalyst mixtures at 65 °C. As seen from the table, the monomer gelation times follow the order: NMDA < NMMA < NMCA ≈ NMSA, indicating that the gelation time is not only determined by the monomer structure, but also the viscosities of the monomers. Thus, the low viscosity NMDA with a more reactive norbornene ring present in the side chain

Table 1
Gel time, extraction data and DMA data for the polymers.

Polymer	Gel Time/s[a]	Soluble(wt%)	E' at 25 °C (Pa)	T_g (°C)[b]	υ_e (mol/m^3)[c]
polyNMSA	1495	13	1.6×10^8	50.0	159
polyNMDA	220	5	5.9×10^8	66.5	307
polyNMMA	889	5	5.5×10^8	70.3	267
polyNMCA	1456	18	7.3×10^8	68.2	331

[a] Gel time was determined at 65 °C.
[b] Glass transition temperatures represent the maxima of the tan δ curves obtained by DMA analysis.
[c] Crosslink densities have been calculated at temperatures 50 °C above the T_g.

Fig. 6. Sample pictures for the polymers (from left to right: polyNMSA, polyNMDA, polyNMMA, and polyNMCA).

exhibits the shortest gelation time, while the highly viscous NMCA with an extra norbornenyl ring present in the side chain shows a much longer gelation time than the other three monomers.

As shown in Fig. 6, all polymer samples are fairly transparent and exhibit essentially the same color as the original oils. Both polyNMDA and polyNMMA exhibit smooth surfaces due to the fact that the extra reactive rings present in the side chain of the oil and the appropriate viscosities of the monomers afford the best incorporation of the polymer chains. However, polyNMSA and polyNMCA exhibit coarse surfaces and lower transparencies, which is probably due to their relatively low crosslink densities and incomplete polymerization of the monomers as discussed later.

To investigate how the polymer structure is affected by the chemical structure of the monomer, all polymer samples have been subjected to Soxhlet extraction to extract the soluble materials present in the final polymers. As shown in Table 1, about 13 wt% of polyNMSA was soluble; while both polyNMDA and polyNMMA afforded only 5 wt% of soluble materials, indicating that the extra norbornene or cyclopentene rings play an important role in increasing the crosslink densities of the resulting thermosets. However, about 18 wt% of polyNMCA was extracted, presumably due to incomplete polymerization of the NMCA. Fig. 7 illustrates the ^{1}H NMR spectra of the soluble materials extracted from the four polymers. Compared to Fig. 2, the peaks between 0.5 and 2 ppm indicated that the soluble fractions mainly consist of the oil fractions. The intensity of the characteristic peaks assigned to the norbornene ring is dramatically decreased in the soluble fractions obtained from polyNMSA, polyNMDA and polyNMMA indicating that almost all of the norbornene rings were ring-opened. However, a significant portion of the norbornene rings remain unreactive in the resulting polyNMCA soluble fraction apparently because the propagation process is hindered by the high viscosity of the monomers.

3.3. Thermal and mechanical properties

Fig. 8 shows the storage modulus (E') and loss factor (tan δ) curves as a function of temperature for the four polymers. All polymers exist in the glassy state at a very low temperature, and the modulus deceases slightly with increasing temperature. Then, a sharp decrease in the E' value is observed in the temperature range from 0 to 100 °C. This corresponds to the primary relaxation process (α) of the resulting thermosets, where a maximum is observed in the loss factor curve, which is taken as the T_g. The

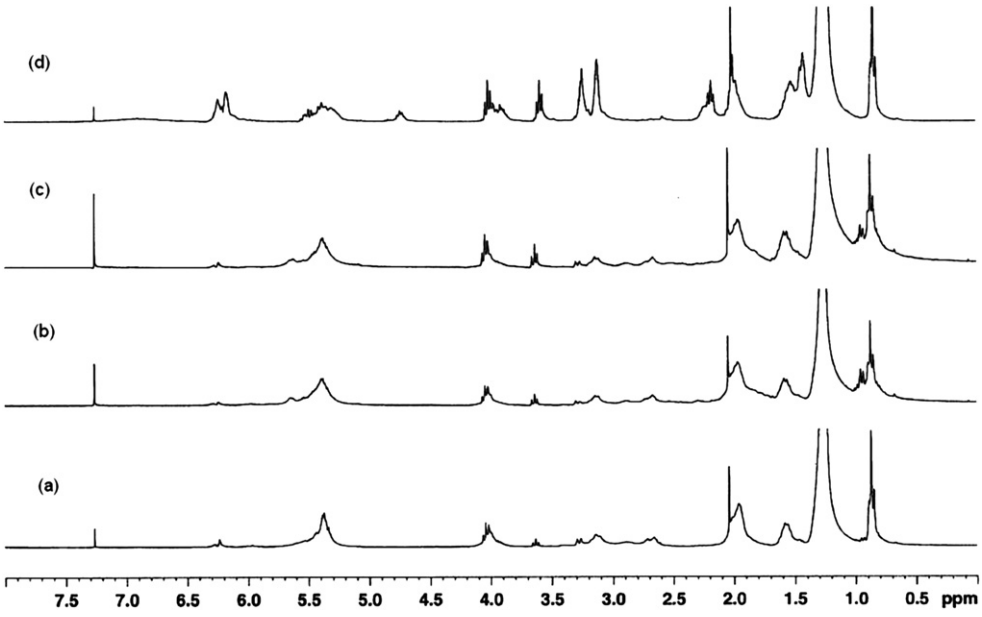

Fig. 7. ^{1}H NMR spectra for the extracted materials from (a) polyNMSA, (b) polyNMDA, (c) polyNMMA, and (d) polyNMCA.

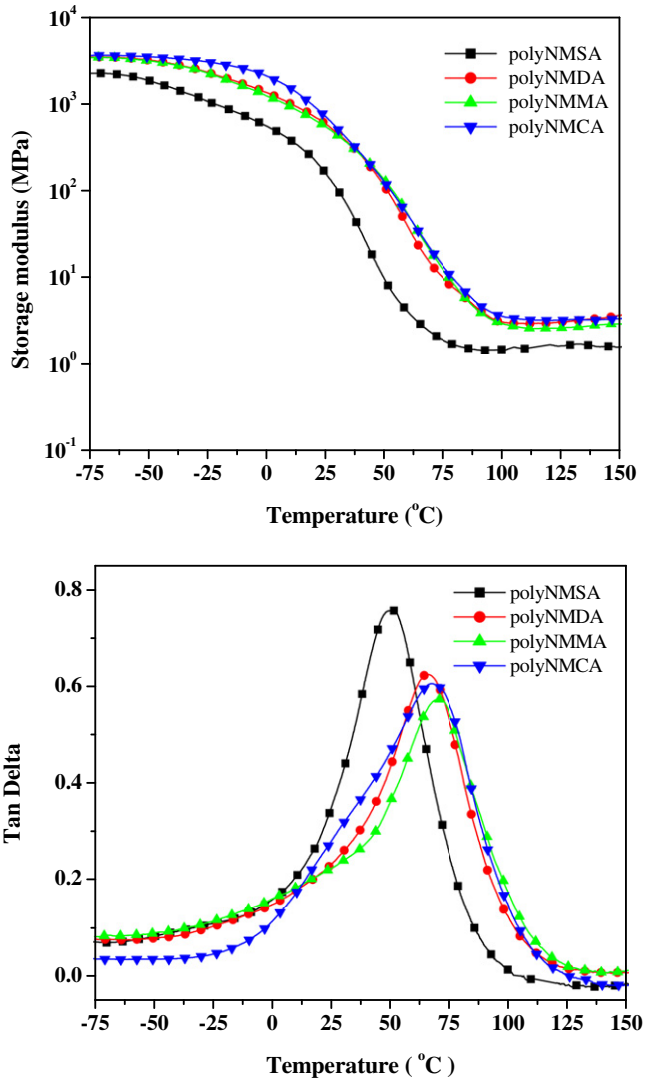

Fig. 8. Tan δ and storage modulus curves for all polymers.

polymer polyNMSA shows a relatively low storage modulus, and its loss factor shows a very sharp relaxation process centered at about 50 °C. When compared with polyNMSA, the E' values of polyNMDA, polyNMMA and polyNMCA were significantly increased over the entire temperature range, due to incorporation of the extra reactive rings present in the side chains. For instance, the E' values for polyNMDA, polyNMMA and polyNMCA at room temperature (Table 1) are approximately 3.7, 3.4 and 4.6 times higher, respectively, than that of polyNMSA. The rubbery plateau modulus can be explained by qualitative consideration of the crosslinking density (ν_e) of the thermosets, according to rubber elasticity theory, using the following equation [27,28]:

$$E' = 3\nu_e RT$$

where E' is the storage modulus at $T_g + 50$ °C in the rubbery plateau, R is the gas constant, and T is the absolute temperature. As seen in Table 1, the thermosets from the monomers with reactive rings in the side chains exhibit much higher crosslink densities then polyNMSA and are typically in the range of 2.6×10^2 – 3.3×10^2 mol/m^3. This indicates that the extra reactive rings in the side chains of the monomers are effectively incorporated into the polymer networks, resulting in higher crosslinked vegetable oil-based thermosets with a resulting enhancement in the rubbery modulus. As molecular motions became more restricted due to the crosslinking, the amount of energy that can be dissipated throughout the polymer specimen decreases dramatically. Therefore, a shift of the loss factor peak to higher temperature is observed for polyNMDA, polyNMMA and polyNMCA as shown in the tan δ - T curves when compared with polyNMSA. The tan δ intensities also diminish. Meanwhile, a significant broadening of the α-relaxation is observed. For the sample polyNMCA, a shoulder peak around 30 °C is observed in the α-relaxation process, which might be attributed to the relaxation of NMCA oligomer-rich phases, because of incomplete polymerization of the viscous NMCA monomers.

Fig. 9 shows the TGA analysis of the resulting thermosets and the corresponding data are summarized in Table 2. As seen in Fig. 9, the polymers are stable up to 150 °C in air and undergo three major thermal degradation processes. The weight loss of the first degradation process from 180 °C to 250 °C approximately equals the soluble fraction as shown in Table 1 and can be attributed to evaporation of any unreacted monomers and oil fragments. In this stage, more than 20% of the overall weight was lost for polyNMCA, because of incomplete polymerization of the NMCA monomers. Less than 10% of the overall weight was lost for polyNMDA and polyNMMA, apparently due to higher crosslinking by the extra

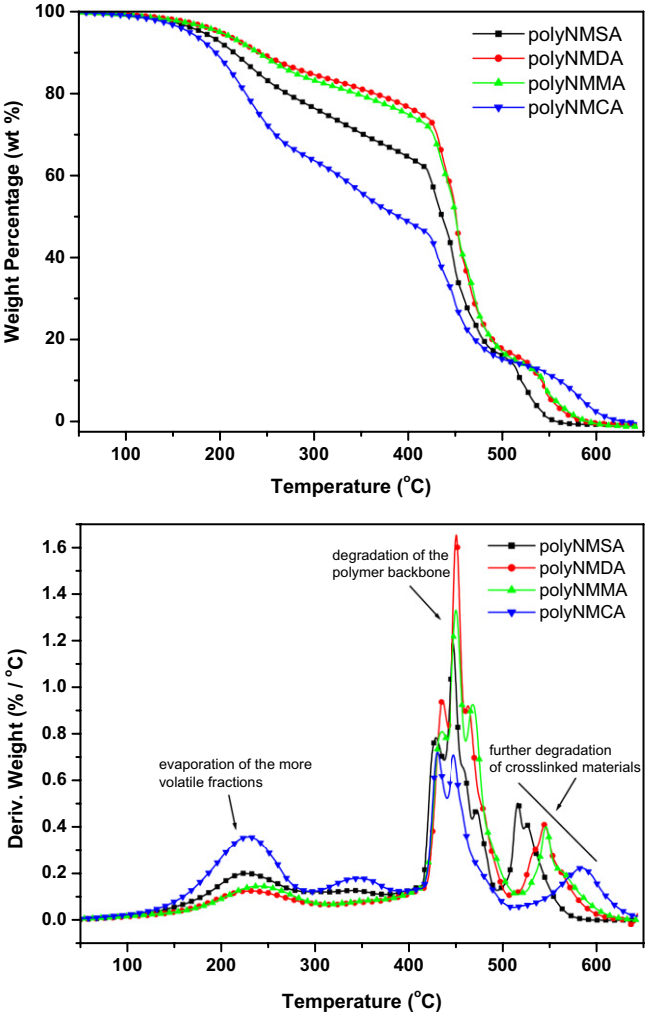

Fig. 9. TGA curves and their derivative curves for all polymers.

Table 2
TGA data and mechanical properties for the polymers.

Polymer	TGA data (°C)			E (MPa)	Mechanical Properties[d]		Toughness (MPa)
	T_{10}[a]	T_{50}[b]	T_{max}[c]		σ_b (MPa)	ε_b (%)	
polyNMSA	215	435	447	–	–	–	–
polyNMDA	243	450	451	311.4 ± 16.7	15.4 ± 0.5	34.5 ± 4.7	4.1 ± 0.6
polyNMMA	240	449	450	154.8 ± 1.1	9.9 ± 0.3	41.0 ± 4.2	2.9 ± 0.3
polyNMCA	196	390	429	–	–	–	–

[a] 10% Weight loss temperature.
[b] 50% Weight loss temperature.
[c] Temperature of maximum thermal degradation.
[d] E = Young's modulus, σ_b = tensile strength, and ε_b = elongation at break.

olefinic rings present in the side chains. The second loss at around 400–500 °C is believed to be caused by decomposition of the polymer backbone. The final loss at around 500–600 °C is indicative of further decomposition of the crosslinked fragments and oxidation of the carbon residue. Table 2 summarizes the interesting parameters from the TGA curves for these thermosets taken from the onset of degradation, which is usually taken as the temperature at which 10% degradation occurs (T_{10}), the midpoint temperature of the degradation (T_{50}), and the maximum degradation temperature (T_{max}). As expected, the samples polyNMDA and polyNMMA exhibit the best thermal stability with similar values of T_{10}, T_{50} and T_{max}. However, lower T_{10}, T_{50} and T_{max} values are observed for polyNMCA due to the incomplete polymerization of the NMCA monomer, because of its high viscosity.

Table 2 also summarizes the mechanical properties for the two most promising thermosets, polyNMDA and polyNMMA. These two samples exhibit Young's moduli ranging from 155 to 310 MPa, tensile strengths ranging from 10 to 15 MPa, elongation at break values in the range of 35–41% and toughness values ranging from 2.9 to 4.1 MPa. It is worth noting that the Young's moduli and tensile strengths of polyNMDA and polyNMMA are comparable to petroleum-based commercial plastics, such as high density polyethylene (HDPE) and poly(norbornene) [29]. The stress-strain curves of the polyNMDA and polyNMMA are shown in Fig. 10. Both polyNMDA and polyNMMA exhibit behaviors typical of ductile plastics. Differing from polyNMMA, polyNMDA shows yielding behavior, followed by strain softening. No strain hardening behavior is observed before the specimen breaks. PolyNMDA exhibits higher values of Young's modulus, tensile strength and toughness than polyNMMA. This is expected, since the extra rigid cyclopentane rings obtained after ring-opening of the norbornene ring present in the NMDA side chains should increase the rigidity and toughness of polyNMDA, whereas the linear polymer chains obtained after the ring-opening of the cyclopentene rings in NMMA would not be expected to increase the modulus and toughness all that much.

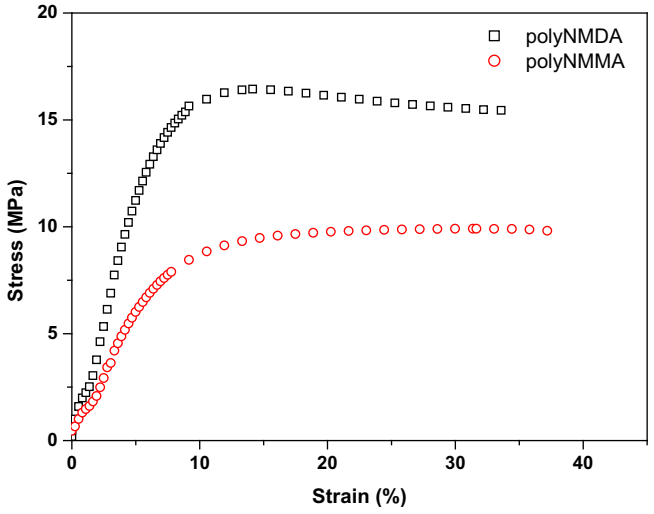

Fig. 10. Stress-strain curves for polyNMDA and polyNMMA.

4. Conclusions

Four different vegetable oil-based monomers, NMSA, NMDA, NMMA and NMCA, have been synthesized from soybean oil, Dilulin, ML189 and castor oil, respectively, followed by esterification with a bicyclic anhydride, and then homopolymerized using the Grubbs 2nd generation ruthenium catalyst to obtain biorenewable thermosets. The differences in the structures of the side chains and the viscosities of the monomers result in different properties in the final thermosets. Compared with polyNMSA, the polyNMDA and polyNMMA thermosets exhibit lower soluble fractions, and higher thermal stabilities and mechanical properties, because of the successful incorporation of the side chain into the polymer matrix to form effective crosslinking. However, polyNMCA affords a higher soluble fraction, and lower thermal stability, resulting from incomplete polymerization of the highly viscous NMCA monomer. Note that polyNMDA and polyNMMA exhibit tensile stress-strain behaviors of ductile plastics with Young's moduli ranging from 155 to 310 MPa, ultimate tensile strengths ranging from 10 to 15 MPa, and percent elongation at break values ranging from 35 to 41%, affording materials comparable to petroleum-based plastics, like HDPE and poly(norbornene). This work provides a new way of utilizing renewable resources to prepare environmentally-friendly bioplastics with high performance.

Acknowledgment

We are grateful for financial support from the Center for Crops Utilization Research (CCUR) at Iowa State University and thankful to Professor Michael Kessler from the Department of Materials Science and Engineering at Iowa State University for the use of his thermal analysis equipments. In addition, we thank Dr. Xia Sheng from the Department of Materials Science and Engineering at Iowa State University for his help with the rheometer tests.

References

[1] Bozell JJ. Clean-Soil Air Water 2008;36:641–7.
[2] Lu YS, Larock RC. ChemSusChem 2009;2:136–47.
[3] Lu J, Khot S, Wool RP. Polymer 2005;46:71–80.
[4] Deng R, Chen Y, Chen P, Zhang LN, Liao B. Polym Degrad Stab 2006;91:2189–97.
[5] Liu WJ, Misra M, Askeland P, Drzal LT, Mohanty AK. Polymer 2005;46:2710–21.
[6] Lu YS, Larock RC. Biomacromolecules 2007;8:3108–14.
[7] Lu YS, Larock RC. Biomacromolecules 2008;9:3332–40.
[8] Li F, Hanson MV, Larock RC. Polymer 2001;42:1567–79.

[9] Kundu PP, Larock RC. Biomacromolecules 2005;6:797–806.
[10] Li FK, Larock RC. Biomacromolecules 2003;4:1018–25.
[11] Li FK, Hasjim J, Larock RC. J Appl Polym Sci 2003;90:1830–8.
[12] Li F, Marks DW, Larock RC, Otaigbe JU. Polymer 2000;41:7925–39.
[13] Rybak A, Meier MAR. ChemSusChem 2008;1:542–7.
[14] Fokou PA, Meier MAR. Macromol Rapid Commun 2008;29:1620–5.
[15] Henna PH, Larock RC. J Appl Polym Sci 2009;112:1788–97.
[16] Henna PH, Larock RC. Macromol Mater Eng 2007;292:1201–9.
[17] Bielawski CW, Grubbs RH. Prog Polym Sci 2007;32:1–29.
[18] Kodali D.R. U.S. Pat. 6,420,322 2002.
[19] Mauldin TC, Haman K, Sheng X, Henna P, Larock RC, Kessler MR. J Polym Sci, Part A: Polym Chem 2008;46:6851–60.
[20] Jones AS, Rule JD, Moore JS, White SR, Sottos NR. Chem Mater 2006;18:1312–7.
[21] Andjelkovic DD, Valverde M, Henna P, Li FK, Larock RC. Polymer 2005;46:9674–85.
[22] Xia Y, Henna PH, Larock RC. Macromol Mater Eng 2009;294:590–8.
[23] Kodali D. R.U.S. Pat. 5,288,805 1994.
[24] Wilson GO, Caruso MM, Reimer NT, White SR, Sottos NR, Moore JS. Chem Mater 2008;20:3288–97.
[25] Sheng X, Lee JK, Kessler MR. Polymer 2009;50:1264–9.
[26] Weng LH, Chen XM, Chen WL. Biomacromolecules 2007;8:1109–15.
[27] Flory PJ. Principles of polymer chemistry. Ithaca: Cornell University Press; 1953.
[28] Ward IM. Mechanical properties of solid polymers. New York: Wiley Interscience; 1971.
[29] Mark JE. Polymer data handbook. New York: Oxford University Press; 1999.